Journal of Materials and Environmental Science
ISSN : 2028-2508
e-ISSN : 2737-890X
CODEN : JMESCN

J. Mater. Environ. Sci., 2025, Volume 16, Issue 3, Page 1109-1121

http://www.jmaterenvironsci.com

Application of *Dichrostachys cinerea* leaves extract as green corrosion inhibitor for aluminium alloy 5083 in NaOH solution

Chimezie N. Achugwo and Nkem B. Iroha*
Department of Chemistry, Federal University Otuoke, Nigeria
**Corresponding author, Email address: irohanb@fuotuoke.edu.ng*

Received *01 May 2025,*
Revised *22 May 2025,*
Accepted *24 May 2025*

Keywords:
- ✓ *Dichrostachys cinerea;*
- ✓ *Aluminium;*
- ✓ *Potentiodynamic polarization;*
- ✓ *Corrosion inhibitor;*
- ✓ *Adsorption isotherm.*

Citation*: Achugwo C. N and Nkem B. Iroha (2025) Application of Dichrostachys cinerea leaves extract as green corrosion inhibitor for aluminium alloy 5083 in NaOH solution, J. Mater. Environ. Sci., 16(3), 1109-1121.*

Abstract: The performance of *Dichrostachys cinerea* (DC) extract as corrosion inhibitor for aluminium in 1 M NaOH solution was investigated using weight loss, electrochemical impedance spectroscopy (EIS), potentiodynamic polarization measurements and scanning electron microscopy (SEM). The results show that DC has a very good corrosion inhibiting effect toward aluminium in 1 M NaOH. Weight loss results revealed that the inhibition efficiency is dependent on the concentration of the extract and the temperature of the system. At 30 °C, the data from weight loss, EIS and polarization studies indicated that DC achieved maximum inhibition efficiencies of 93.6%, 91.2%, and 90.4%, respectively at a concentration of 2.5 g L^{-1}. Polarization measurements indicated that DC has a mixed-type inhibitory behaviour, reducing both the cathodic/anodic partial reactions. The adsorption process followed the Langmuir adsorption isotherm model at all studied temperatures between 30 and 50 ºC. SEM images revealed the formation of a protective adsorbed layer on the aluminium surface in the alkaline solution.

1. Introduction

Aluminium and its alloys are widely used in a broad range of applications such as construction of aircraft, fabrication of pipes, cars, and marine parts due to their low density and high mechanical strength (Udensi *et al.* 2021, Raghavendra 2020). It is, therefore, very important to prevent this metal from corrosion. The study of the corrosion behaviour of aluminium in various corrosive media and its corrosion inhibition has continued to attract considerable attention because of the many vital applications of the metal. Corrosion inhibitors have been shown to be one of the most cost effective and practical methods of fighting corrosion (Iroha *et al.* 2023; Merimi *et al.* 2021; Emori *et al.* 2020; Bouklah *et al.* 2006). Corrosion inhibitors can effectively reduce corrosion, suppressing the high metal dissolution rate (Al-Rashed and Abdel Nazeer 2022). A good inhibitor should have a great affinity for being adsorbed on metal surfaces and, hence, inhibit it through strong binding with metallic d-orbitals (Umoren and Eduok, 2016). The inhibition basically has to do with the displacement of water molecules on the surface of metals by organic compounds inherent in the inhibitors, via physical and/or chemical adsorption, depositing a protective film that reduces further dissolution.

Application of toxic corrosion inhibitors has been restricted and as a result, researchers have focused on eco-friendly inhibitors like plant extracts (Ji *et al.* 2015; James and Iroha 2019; Keramatinia, 2019; Iroha *et al.* 2012; Nahle *et al.* 2021; Salmasifar *et al.* 2021; James and Iroha 2022; Haddadi *et al.* 2019; Aouniti *et al.* 2013), biopolymers (Biswas *et al.* 2019; Eddy *et al.* 2014; Eid *et al.* 2015; El Azzouzi *et al.* 2022), etc, in their attempts to mitigate corrosion damages. The increasing use of plant extracts in the corrosion inhibition of metal and alloys in various environments is probably due to their biodegradability, cheap cost, non-toxic nature, ecologically friendly, and high availability (Abdelshafeek *et al.* 2022; Iroha and Madueke 2018). Furthermore, most plant extracts have complex chemical compositions and corrosion inhibitory properties due the presence of phenols, flavonoids, terpenes, tannins, essential oils, and carboxylic acids (Eddahhaoui *et al.* 2024; Iroha and Nnanna 2020). In recent times, many natural products like *Treculia africana* leaves extract (Udensi *et al.* 2021), *Ajuga orientalis* L. Extract (Abu-Orabi *et al.* 2024), *Tribulus terrestris* Plant Extract (Chaudhary and Tak 2022), *Conocarpus erectus* extract (Fouda *et al.* 2021) and *Tagetes erecta* leaf extract (Obruche *et al.* 2019) were investigated as green inhibitors for aluminium corrosion. It was found that these molecules adsorb spontaneously on aluminium surface mainly by physical adsorption and inhibition efficiency varied from 80 to 90 %.

The aim of this research is to investigate the inhibition properties of Dichrostachys cinerea (DC) on the dissolution of Aluminium in 1 M NaOH solution using chemical and electrochemical methods. The surface morphology of Aluminium was investigated before and after inhibition. DC, a deciduous low thorny tree or shrub that produces bicoloured fragrant flowers was chosen as a potential eco-friendly corrosion inhibitor for aluminium due to the presence of various phytoconstituents, such as Saponins, flavonoids and phenols (Shandukani *et al.* 2018).

2. Methodology

2.1 Sample preparation

Aluminium plates with dimension of 3 x 3 x 0.2 cm were cut into coupons, with holes drilled at the top to aid during dipping in the NaOH solutions, abraded by emery papers at different grit sizes from 400 to 1200, rinsed with double distilled water, degreased in acetone to get rid of all possible impurities, dried with filter paper, weighed. The corrosive solution was 1 M NaOH prepared from analytical grade NaOH (MERCK) and double-distilled water.

2.2 Preparation of Plant Extract

Leaves of Dichrostachys cinerea were washed under running water, dried using a fluidized bed dryer for 1 h and grinded to powder to give 150 gm of powdered material. The DC inhibitor was extracted by soaking in 70 % methanol (250 ml) for 48 h at room temperature. The methanolic extract of the sample was then concentrated to nearly dryness utilizing the rotary evaporator at 45 ºC to achieve the crude extract. The concentration of the inhibitor test solutions was calculated in the range of 0.5 g L^{-1} to 2.5 g L^{-1}.

2.3 Gravimetric measurements

Gravimetric tests were performed as described elsewhere (Iroha *et al.* 2022). Prepared Aluminium specimens were immersed in 200 mL of 1 M NaOH with and without various concentrations of DC leaves extract at 30 ºC, 40 ºC, and 50 ºC. The corrosive systems temperatures were controlled by an air thermostat. After 3 h immersion, the aluminium specimens were retrieved from the test solutions, washed in distilled water, dried, and re-weighed. The weight loss data, calculated from the initial and

final weights of each specimen were gained from the average value of three parallel samples in 1 M NaOH with DC extract at various concentrations. This was further used to compute corrosion rate (CR; mg cm^{-2} h^{-1}) and corrosion inhibition efficiency (E_{WL}%) from the following equations:

$$CR = \frac{\Delta W}{At} \quad \textbf{Eqn. 1}$$

$$\%IE_{WL} = \frac{CR_0 - CR_i}{CR_0} \times 100 \quad \textbf{Eqn. 2}$$

where ΔW represents aluminium sample weight loss (mg) in time t (h) and A denotes surface area (cm^2). The symbols CR_0 and CR_i stands for corrosion rate in blank NaOH solution and inhibited NaOH solution respectively.

2.4 Electrochemical measurements

Electrochemical experiments were undertaken using the conventional three-electrode double-walled glass cell with a saturated calomel reference electrode (SCE), a platinum disc as counter electrode (CE) and Aluminium used as working electrode (WE), with the surface area of 0.85 cm2 exposed to the electrolyte. Prior to the electrochemical measurements, the WE was immersed in the test solution at open circuit potential (OCP) for 25 min at 30 ºC, till steady state is obtained. All measurements were performed with a PGSTAT potentiostat/galvanostat controlled by a personal computer using Nova 1.5 software. Potentiodynamic polarization curves were scanned in the potential ranges of -250 to 250 mV with respect to OCP at a scan rate of 1 mV/s. EIS measurements were performed at OCP utilizing ±10 mV AC perturbation (rms) between 10 kHz to 5 mHz frequency range after a stationary state was achieved. Tests were repeated three times to check the results reproducibility.

2.5 Surface Investigation Technique

The mild steel specimens were submerged in 200 mL of 1 M NaOH solution containing optimum concentrations (2.5 g L-1 of DC) for 3 h. After the expiration of 3 h, the specimens were retrieved and dried. The surface morphological examination of the Aluminium after 3 h immersion in 1 M NaOH solution without and with various inhibitor concentrations was performed utilizing ZEISS EVO scanning electron microscope.

3. Results and Discussion

3.1 Polarization Tests

Figure 1 shows the potentiodynamic polarization curves for Aluminium in 1 M NaOH solution with and without different concentrations of DC at 30 ºC. Inspection of the figure indicates that the cathodic and anodic curves exhibited Tafel-type behaviour. Important polarization parameters deduced from the figure, such as corrosion potential (E_{corr}), corrosion current density (i_{corr}), cathodic (βc) and anodic (βa) Tafel slopes and the inhibition efficiencies are listed in **Tables 1**. The inhibition efficiency ($\%IE_{PDP}$) was computed according to the equation.

$$\%IE_{PDP} = \frac{i^0_{corr} - i_{corr}}{i^0_{corr}} \times 100 \quad \textbf{Eqn. 3}$$

Where i^0_{corr} and i_{corr} are the corrosion current densities in the absence and presence of the DC extract, respectively. **Figure 1** reveals that, on adding DC to the reference electrolyte, the polarization curves shift to reduced current densities. Furthermore, adding DC to the 1 M NaOH solution reduces the

anodic and cathodic current densities, which indicates that DC inhibits both the dissolution of the aluminium and the cathodic hydrogen evolution (Zhang *et al.* 2021, Iroha *et al.* 2021). All scans exhibited similar polarization behaviour over the range of potential examined, indicating that similar electrochemical reactions took place after adsorption of DC inhibitor onto the aluminium surface. **Table 1** indicates that the i_{corr} decreases and $\%IE_{PDP}$ increases as the inhibitor concentration increases. This clearly indicates that DC is adsorbed on the aluminium surface to form protective film thereby reducing the exposed active sites on the aluminium surface (Singh *et al.* 2013, Iroha *et al.* 2022, Nadi *et al.* 2019).

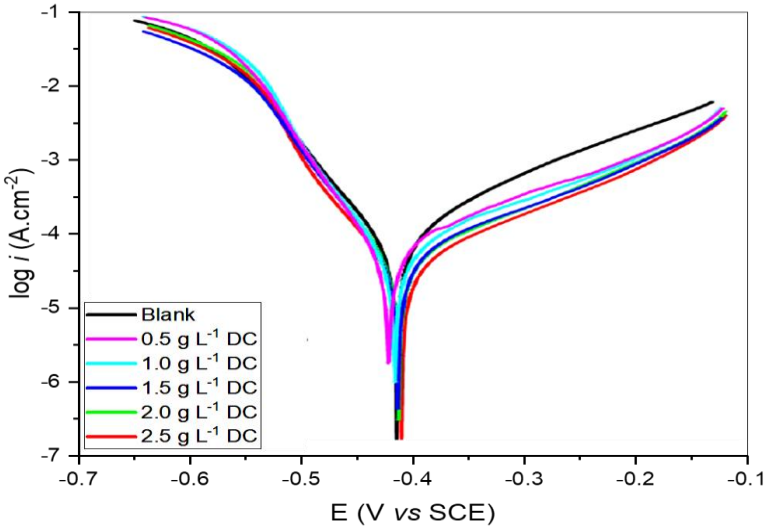

Figure 1. Tafel polarization curves for aluminium specimen immersed in 1 M NaOH in the absence and presence of different DC concentrations.

Table 1. Polarization parameters for aluminium specimen immersed in 1 M NaOH in the absence and presence of different DC concentrations.

Conc. (g L^{-1})	E_{corr} (mV/SCE)	i_{corr} (µA cm^{-2})	β_a (mV dec^{-1})	$-\beta_c$ (mV dec^{-1})	IE_{PDP} (%)
Blank	-416.3	582.2	131.9	154.7	-
0.5	-427.7	269.3	115.3	158.2	53.7
1.0	-417.0	227.4	112.6	165.1	60.9
1.5	-414.9	152.7	117.0	162.6	73.8
2.0	-413.6	110.6	121.5	167.2	81.0
2.5	-408.3	55.9	119.6	166.3	90.4

3.2 Electrochemical impedance spectroscopic (EIS) studies

Electrochemical impedance spectroscopy is considered a powerful non-destructive diagnostic technique in the study of corrosion. EIS technique was employed at 303 K to examine the corrosion mechanism of aluminium in 1 M NaOH solution in the absence and presence of DC. **Figure 2** shows the Nyquist plot of aluminium in 1 M NaOH with various concentrations of DC at 303 K. The Nyquist plots consist of depressed capacitive semicircle loops which indicate that the adsorption of DC happened by masking the aluminium surface by their molecules (Fontana and Staehle 1970). In Nyquist plot, semicircle indicates that charge transfer phenomenon controls the corrosion process of the aluminium and its inhibition (Anadebe *et al.* 2022, Iroha *et al.* 2025). The diameter of semicircle increases with increase in inhibitor concentration which indicates that the inhibitor protects the metal from corrosion (Aliyari *et al.* 2024, Iroha and Dueke-Eze 2023). However, no obvious change was

observed in the shape and nature of the Nyquist curves with DC, suggesting that the introduction of DC into the 1 M NaOH solution did not alter or modify the corrosion phenomenon at the Al/solution interface. Making use of the nova 2.1.4 software, the most appropriate equivalent circuit was employed to simulate the EIS findings as depicted in **Figure 3**, consisting of a series connection between the solution resistance (Rs) and these impedance components, together with a parallel connection between the constant phase element (CPE) and the charge transfer resistance (R_{ct}). The EIS parameters evaluated from the equivalent circuit are listed in **Table 2**. To account for the surface inhomogeneity caused by surface roughness, the CPE is used in place of a pure capacitor. The impedance of a CPE is mathematically expressed as (Merimi *et al.* 2024, Abeng *et al.* 2023)

$$Z_{CPE} = [Q(j\omega)^n]^{-1} \qquad \textbf{Eqn. 4}$$

where ω represents angular frequency, Q is the constant and n is the CPE power with values ranging between 0.5 and 1. When n = 1, the CPE describes an ideal capacitor with Q equal to the capacitance (C). For 0.5 < n < 1, the CPE describes a distribution of dielectric relaxation times in frequency space, and when n = 0.5 the CPE represents a Warburg impedance. The data presented in **Table 2** indicate that the R_{ct} values when DC inhibitor was introduced are higher than the value of the R_{ct} for blank. This increase in R_{ct} values is attributed to the formation of protective film of DC at the metal/solution interface. The C_{dl} value decreased on increasing the concentration of DC due to an increase in the thickness of electrical double layer at Al/solution interface (Abdulazeez *et al.* 2022, Chokor *et al.* 2022). The results obtained from polarization test and EIS methods are in good agreement.

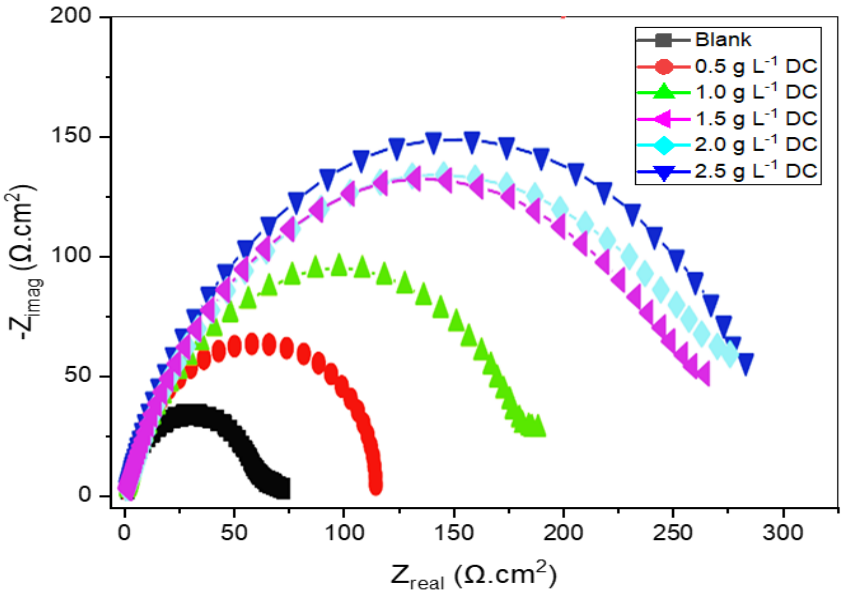

Figure 2. Nyquist plot for corrosion of aluminium in 1 M NaOH without and with various concentrations of DC at 303 K.

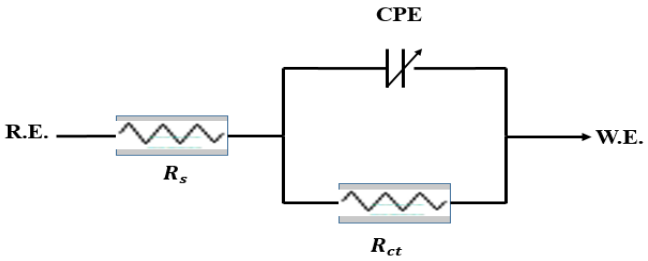

Figure 3. Nyquist plots for aluminium in 1 M NaOH without and with various concentrations of DC at 303 K

Table. Electrochemical impedance parameters for aluminium in 1 M NaOH without and with various concentrations of DC at 303 K

Conc. (g L^{-1})	R_s (Ω cm^2)	R_{ct} (Ω cm^2)	C_{dl} (µF cm^{-2})	n	IE_{EIS} (%)
Blank	1.68	18.6	227.1	0.872	-
0.5	1.20	39.4	105.3	0.885	52.8
1.0	1.47	52.5	87.4	0.937	64.6
1.5	1.52	84.3	42.9	0.948	77.9
2.0	1.79	117.3	21.0	0.963	84.1
2.5	1.91	211.7	12.6	0.974	91.2

3.3 Weight loss measurement

The results of weight loss measurements in the absence and presence of various DC concentrations are shown in **Figure 4 (a, b)**. Scrutiny of the results revealed that, as DC concentration is increased, the CR decreased (**Figure 4a**) and inhibition efficiency, E_{WL}% increased (**Figure 4b**), likely because of the effective defense of the metal surface leading the retardation of the aluminium dissolution process.

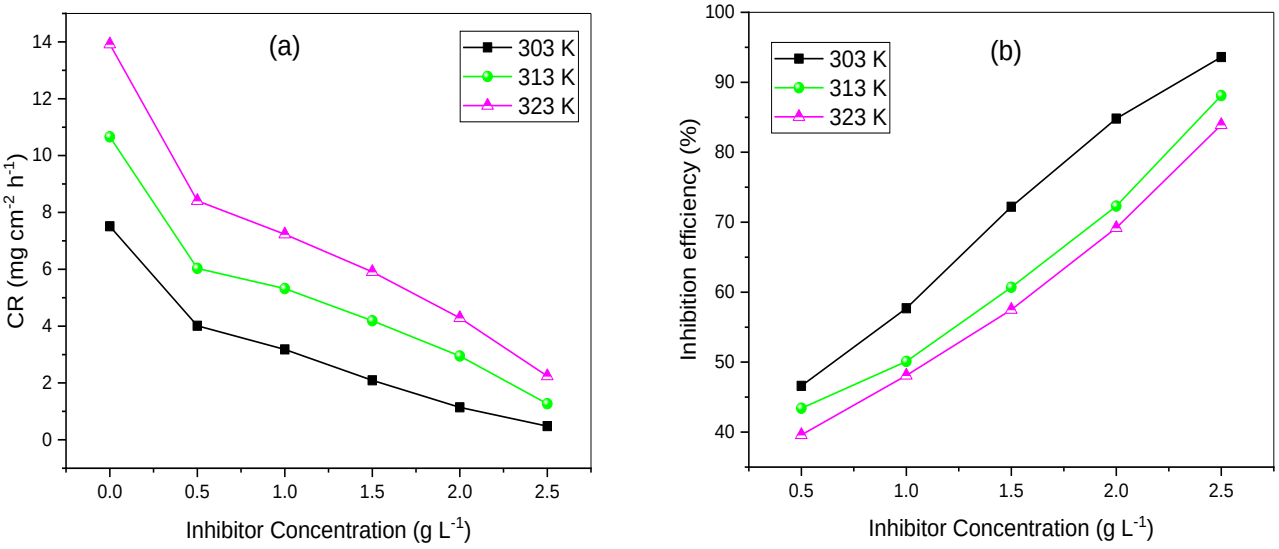

Figure 4. (a) CR versus concentration and (b) Inhibition efficiency versus concentration for aluminium corrosion in 1 M NaOH solution, containing 0 to 2.5 g/L of DC extracts after 3 h.

The E_{WL}% was found to be the highest at an optimum DC concentration of 2.5 gL^{-1}, which is likely due to the adsorption of DC compound at the mild steel surface (Nwosu and Muzakir 2016, Iroha and Dueke-Eze 2021). This also shows that by increasing the concentration of DC more of its molecules were adsorbed on the surface of the mild steel, resulting to an increased θ. This behaviour reflects the inhibitory effect of DC against aluminium corrosion in 1 M NaOH environment.

3.4 Adsorption isotherm

The nature of adsorption of a compound can be assured by fitting the experimental data into different adsorption isotherms. In this study, the adsorption parameters were best fitted in Langmuir isotherm. The adsorption equilibrium constant K_{ads} for the studied DC extract was evaluated by utilizing **Eqn. 5** and the values listed in **Table 3**.

$$\frac{C_{inh}}{\theta} = \frac{1}{K_{ads}} + C_{inh} \qquad \textbf{Eqn. 5}$$

where C_{inh} is the inhibitor concentration, θ is the degree of surface coverage and K_{ads} is the adsorption equilibrium constant. The Langmuir isotherm plot is shown in **Figure 5**, with a correlation coefficient (R^2) close to unity. The adsorption parameters obtained from the Langmuir's plot is shown in **Table 3**. The Kads values were deduced from the intercept and the change in Gibb's free energy (ΔG_{ads}) for the adsorption process was computed utilizing the equation:

$$\Delta G^0_{ads} = -RT \ln(55.5 K_{ads}) \qquad \textbf{Eqn. 6}$$

where R represents universal gas constant, T is absolute temperature and 55.5 is the molar concentration of water in solution. The high value of K_{ads} obtained, indicates that the molecules of DC are strongly adsorbed on the aluminium surface (Myung et al. 2003, Mohamme et al. 2012, Rani and Selvaraj 2010, Iroha and Nnanna 2021). However, the values of K_{ads} were found to decrease with increase in temperature, with suggest reduced strength of DC adsorption on the aluminium surface.

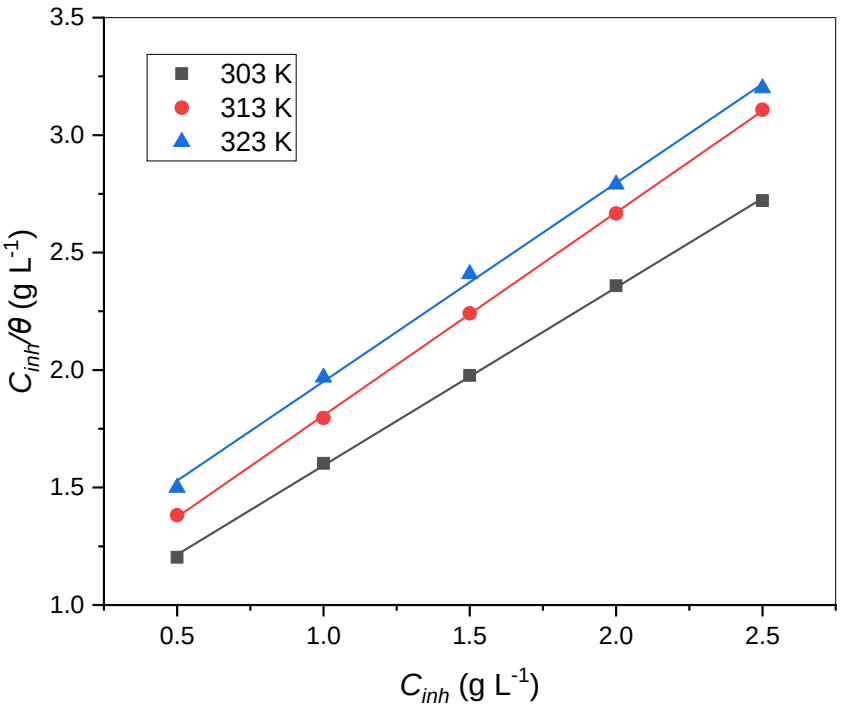

Figure 5. Langmuir isotherm model for DC adsorption on aluminium surface in 1 M NaOH at different temperatures.

The ΔG_{ads} value is mostly used to classify the adsorption process as chemisorption, physisorption or a combination of both. Values of ΔG_{ads} around −20 kJmol^{-1} or less negative suggests an adsorption process involving electrostatic interactions between the charged metal surface and the charged molecules, termed physisorption. In contrast, values of ΔG_{ads} around −40 kJmol^{-1} or more negative suggest an involvement of charge transfer or sharing from inhibitor molecules to the metal surface, and the adsorption process is termed chemisorption (Bentiss et al. 2011, Ahamad et al. 2010).

The existence of data in the literature confirmed the presence of various components as described by El-Sharawy *et al.*, (2017). They were identified as: apigenin-7-O-apiosyl (1 → 2) glucoside **(1)** (Li et al., 1997), chrysoeriol-7-O-apiosyl (1 → 2) glucoside **(2)** (Lin et al., 2007) and the major compound clovamide (N-caffeoyl-LDOPA) **(3)** (Sanbongi et al., 1998), were isolated for the

first time from the plant. Quercetin-3-O-rhamnopyranoside **(4)** (Zeid et al., 2009), myricetin-3-O-rhamnopyranoside **(5)** (Kassem et al., 2016), myricetin-3-O-glucopyranoside **(6)** (Zeid *et al.*, 2009), quercetin3-O-glucopyranoside **(7)** (Zeid *et al.*, 2009), myricetin **(8)** (Kassem et al., 2016), apigenin **(9)** (Marzouk *et al.*, 2016) and kaempferol **(10)** (Marzouk *et al.*, 2016) were previously reported to occur in the plant (Zeid *et al.*, 2009), which can be presented in Figure 6. These components, rich in aromatic rings, heteroatoms, ketones, etc, efficiently adsorb on the metal surface to explain the high efficiency obtained (≈90%). They act competitively or cooperatively to suggest the intermolecular synergistic effect as proposed by several authors (Haddou *et al.*, 2025; Lrhoul *et al.*, 2023; Zeid *et al.*, 2009).

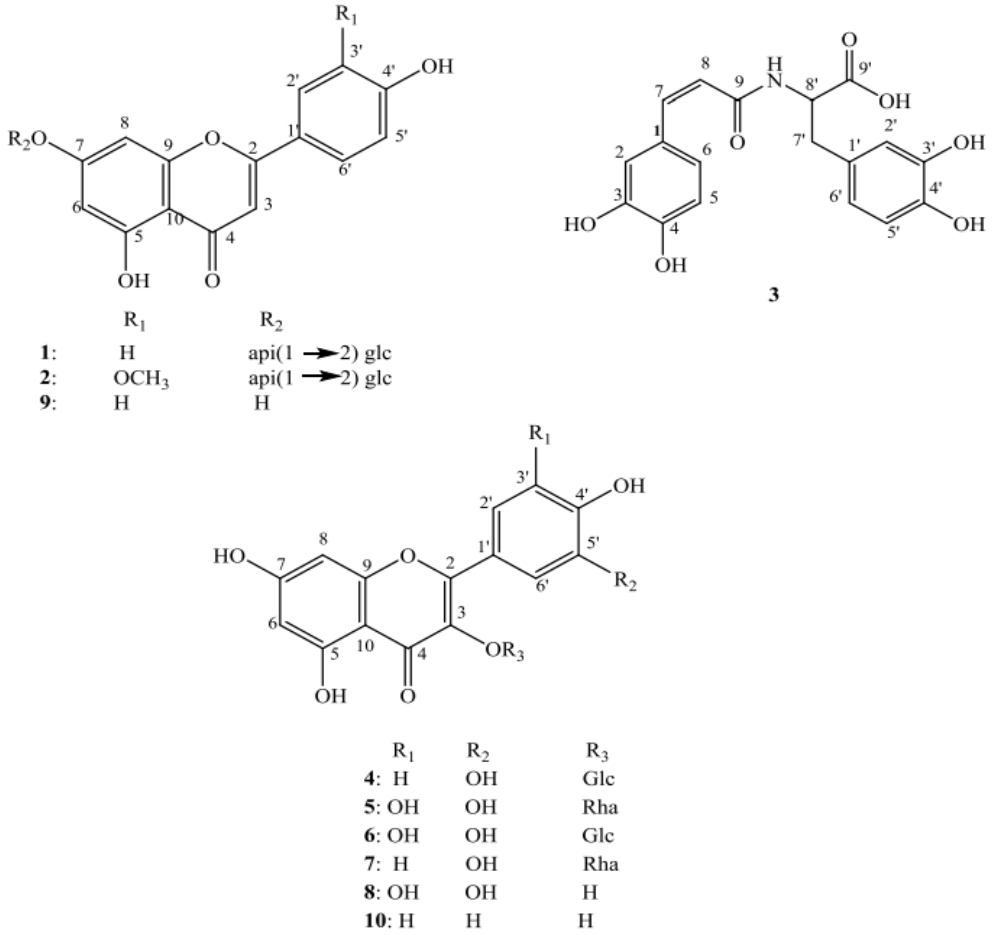

Figure 6. Chemical Structures of the isolated compounds from *Dichrostachys cinerea* (El-Sharawy *et al.*, 2017)

Table 4. Langmuir isotherm parameters for DC adsorption on aluminium surface in 1 M NaOH at different temperatures.

Temp. (K)	R^2	Slope	K_{ads} (L g^{-1})
303	0.9997	0.7583	28.29
313	0.9999	0.8643	15.85
323	0.9998	0.8443	12.47

3.5 Scanning Electron Microscope (SEM)

Surface analyses for aluminium corrosion in 1 M NaOH solution without and with 2.5 gL^{-1} DC inhibitor were performed by SEM. **Figure 6 (A, B)** shows the SEM pictures of aluminium surface

exposed to the 1 M NaOH for 6 h without and in presence of DC. In **Figure 6A**, the surface shows visible severe corrosion in the absence of DC inhibitor. **Figure 6B** reveals a rather smooth aluminium surface with no rusted spots, appearing to be almost unaffected by corrosion. This is due to the adsorption of DC molecules forming a thin protective film of inhibitors on the Al surface. This film is responsible for the effective inhibition by this inhibitor.

.

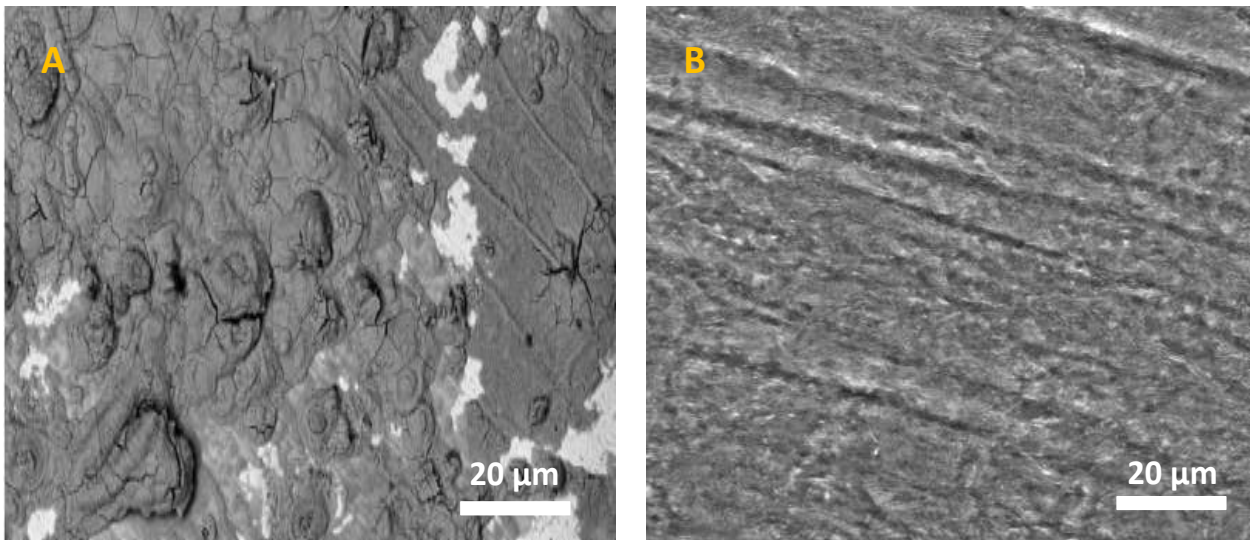

Figure 6. SEM images for aluminium surface immersed in (A) 1 M NaOH without DC inhibitor and (B) 1 M NaOH with 2.5 gL^{-1} DC inhibitor.

Conclusion

The studied DC leaves extract proved to be a good corrosion inhibitor for aluminium in 1 M NaOH solution. The inhibition efficiency increases with increase in inhibitor concentration but decrease with temperature. Tafel data reveal that the studied DC inhibitor acts as a mixed type, retarding both anodic and cathodic processes without changing the mechanism of corrosion. EIS results show that the use DC extract significantly increases the charge transfer resistance and decreases the double layer capacitance, indicating that the adsorption leads to the formation of a protective film on the aluminium surface. The adsorption of the inhibitor on aluminium surface followed Langmuir adsorption isotherm and it involves a combination of physisorption and chemisorption mechanisms. The data obtained from weight loss, potentiodynamic polarization and electrochemical impedance spectroscopy are in good agreement.

Acknowledgement: Department of Chemistry, Federal University Otuoke is acknowledged.
Disclosure statement: *Conflict of Interest:* The authors declare that there are no conflicts of interest.
Compliance with Ethical Standards: This article does not contain any studies involving human or animal subjects.

References

Abdelshafeek K. A., Abdallah W. E., Elsayed W. M., Eladawy H. A. & El-Shamy A. M. (2022) Vicia faba peel extracts bearing fatty acids moieties as a cost-effective and green corrosion inhibitor for mild steel in marine water: computational and electrochemical studies. *Scientific Reports*, 12, 20611. https://doi.org/10.1038/s41598-022-24793-3.

Abdulazeez I., Peng Q., Al-hamouz O.C.S., Khaled M., Al-saadi A.A. (2022) Evaluation of the inhibition

performance of piperazine-based polyurea towards mild steel corrosion: The role of keto-enol tautomerization, J. Mol. Struct. 1248, 131485. https://doi.org/10.1016/j.molstruc.2021.131485

Abeng F.E, Ita B.I, Anadebe V.C, Chukwuike V.I, Etiowo K.M, Nkom P.Y, Ekerenam O.O., Iroha N.B., Ikot I.J. (2023) Multidimensional insight into the corrosion mitigation of clonazepam drug molecule on mild steel in chloride environment: Empirical and computer simulation explorations. *Results in Engineering*, 17, 100924. https://doi.org/10.1016/j.rineng.2023.100924

Abu-Orabi F. M., Abu-Orabi S. T., Fodeh O. A., Algethami F. K., Rawashdeh A. M. M., Bataineh T. T., Al-Mazaideh G. M., Al-Qudah M. A. (2024) Ajuga orientalis L. Extract as a Green Corrosion Inhibitor of Aluminum in an Acidic Solution: An Experimental and DFT Study. *Metals*,14(11), 1227; https://doi.org/10.3390/met14111227

Ahamad I., Prasa R., Quaraishi M.A. (2010) Experimental and theoretical investigation of adsorption of fexofenadine at mild steel/hydrochloric acid interface as corrosion. *J. Solid State Electr.,* 14, 2095–2105.

Aliyari D., Mahdavian M., Ramezanzadeh B. (2024) Zinc–cobalt bimetallic metal-organic framework (Zn/Co-MOF) nanoparticles as potent pH stimuli anti-corrosive agent for development of a self-healable epoxy composite coating. *Mater. Today* Chem. 38, 102105.

Al-Rashed O., Abdel Nazeer A. (2022) Effectiveness of Some Novel Ionic Liquids on Mild Steel Corrosion Protection in Acidic Environment: Experimental and Theoretical Inspections. *Materials*, 15, 2326. https://doi.org/10.3390/ma15062326

Anadebe V.C., Chukwuike V.I., Selvaraj V., Pandikumar A., Barik R.C. (2022) Sulfur-doped graphitic carbon nitride (S-g-C3N4) as an efficient corrosion inhibitor for X65 pipeline steel in CO2-saturated 3.5% NaCl solution: Electrochemical, XPS and Nanoindentation Studies. *Process Saf. Env. Prot.* 164, 715-728.

Aouniti A., Khaled K.F., Hammouti B. (2013), Correlation Between Inhibition Efficiency and Chemical Structure of Some Amino Acids on the Corrosion of Armco Iron in Molar HCl, *Int. J. Electrochem. Sci.,* 8(4), 5925-5943

Bentiss F., Mernari B., Traisnel M., Vezin H., Lagrenée M. (2011) On the relationship between corrosion inhibiting effect and molecular structure of 2,5-bis(n-pyridyl)-1,3,4-thiadiazole derivatives in acidic media: AC impedance and DFT studies. *Corr. Sci.,* 53, 487–495.

Biswas A., Das D., Lgaz H., Pal S., Nair U. G. (2019) Biopolymer dextrin and poly (vinyl acetate) based graft copolymer as an efficient corrosion inhibitor for mild steel in hydrochloric acid: Electrochemical, surface morphological and theoretical studies. *J. Mol. Liq*., 275, 867–878.

Bouklah M., Ouassini K., Hammouti B., El Idrissi A. (2006), Corrosion inhibition of steel in sulphuric acid by pyrrolidine derivatives, *Appl. Surf. Sci.,* 252, 2178-2185. https://doi.org/10.1016/j.apsusc.2005.03.177

Chaudhary S. & Tak R. K. (2022). Natural Corrosion Inhibition and Adsorption Characteristics of Tribulus terrestris Plant Extract on Aluminium in Hydrochloric Acid Environment. *Biointerface Research in Applied Chemistry Platinum Open Access Journal*, 12(2), 2603 - 2617 https://doi.org/10.33263/BRIAC122.26032617

Chokor A. A., Dueke-Eze C. U., Nnanna L. A., Iroha N. B. (2022) Adsorption, electrochemical and theoretical studies on the protective effect of N-(5-bromo-2-hydroxybenzylidene) isonicotinohydrazide on carbon steel corrosion in aggressive acid environment. *Safety in Extreme Environments*, 4 (1), 35-45. https://doi.org/10.1007/s42797-022-00050-8

Eddahhaoui F., Najem A., Elhawary M., Boudalia M., Campos O. S., Tabyaoui M., Garcia A. J., Bellaouchou A., Amin H.M.A. (2024) Experimental and computational aspects of green corrosion inhibition for low carbon steel in HCl environment using extract of Chamaerops humilis fruit waste. *Journal of Alloys and Compounds* 977, 173307

Eddy N.O., Ameh P.O., Odiongenyi A.O. (2014) Physicochemical characterization and corrosion inhibition potential of Ficus benjamina (FB) gum for aluminum in 0.1 M H_2SO_4. *Port. Electrochim. Acta*, 32, 183-197

Eid S., Abdallah M., Kamar E. M., El-Etre A. Y. (2015) Corrosion inhibition of aluminum and aluminum silicon alloys in sodium hydroxide solutions by methyl cellulose. *J. Mater. Environ. Sci*., 6, 892-901.

El Azzouzi M., Azzaoui K., Warad I., *et al*. (2022), Moroccan, Mauritania, and Senegalese gum Arabic variants as green corrosion inhibitors for mild steel in HCl: Weight loss, Electrochemical, AFM and XPS studies, *Journal of Molecular Liquids,* 347, 118354, https://doi.org/10.1016/j.molliq.2021.118354

El-Sharawy R.T., Elkhateeb A., Marzouk M.M., Abd El-Latif R.R., Abdelrazig S.E., El-Ansari M.A. (2017). Antiviral and antiparasitic activities of clovamide: the major constituent of Dichrostachys cinerea (L.) Wight et Arn. *J App Pharm Sci*, 7 (09), 219-223.

Emori W., Zhang R.H., Okafor P.C., Zheng X.W., He T., Wei K., Lin X.Z., Cheng C.R. (2020) Adsorption and corrosion inhibition performance of multi-phytoconstituents from Dioscorea septemloba on carbon steel in acidic media: Characterization, experimental and theoretical studies. *Colloids and Surfaces A: Physicochemical and Engineering Aspects*, 590, 1-13. https://doi.org/10.1016/j.colsurfa.2020.124534.

Fontana M.G., Staehle R.W. (1970) Advances in Corrosion Science and Technology; Springer US: Boston, MA, USA, ISBN 978-1-4615-8254-0.

Fouda A. S., Tilp A. H. & Al-Bonayan A. M. (2021). Conocarpus erectus extract as an eco-friendly corrosion inhibitor for aluminum in hydrochloric acid solution. *Biointerface Research in Applied Chemistry*, 11(3), 10325 – 10340: https://doi.org/10.33263/BRIAC113.1032510340

Haddadi S. A., Alibakhshi E., Bahlakeh G., Ramezanzadeh B., Mahdavian M. A. (2019) detailed atomic level computational and electrochemical exploration of the Juglans regia green fruit shell extract as a sustainable and highly efficient green corrosion inhibitor for mild steel in 3.5 wt% NaCl solution. *J. Mol. Liq.* 284, 682–699.

Haddou S., Zaidi K., Dagdag O., Hbika A., Mahraz M.A., et al., (2025) Theoretical and Electrochemical Evaluation of Cannabis Sativa L. Extracts as Corrosion Inhibitors for Mild Steel in Acidic Medium, *Chemistry Open*, 14(5), e202400273, https://doi.org/10.1002/open.202400273

Iroha N. B., Akaranta O., James A. O. (2012) Corrosion inhibition of mild steel in acid media by red peanut skin extract-furfural resin. *Advances in Applied Science Research* 3 (6), 3593-3598

Iroha N. B., Dueke-Eze C. U. (2021) Experimental studies on two isonicotinohydrazide-based schiff bases as new and efficient inhibitors for pipeline steel erosion corrosion in acidic cleaning solution. *Chemistry Africa* 4 (3), 635-646. https://doi.org/10.1007/s42250-021-00252-w

Iroha N. B., Dueke-Eze C. U. (2023). A novel Schiff base of pyridine-2-amine derivative as an effective inhibitor of the dissolution of N80 pipeline steel in 1 M HCl. *Safety in Extreme Environments.* https://doi.org/10.1007/s42797-023-00082-8

Iroha N. B., Dueke-Eze C. U., Anadebe V. C., Maduelosi N. J., Thomas R., Ebenso E. E. (2025) Assessment of a new benzylidene-based corrosion inhibitor for X60 carbon steel in 1 M HCl medium: Experimental and computational studies. *Results in Surfaces and Interfaces*, 19, 100510

Iroha N.B, Dueke-Eze C.U, Fasina T.M, Anadebe V.C, Guo L. (2022) Anticorrosion activity of two new pyridine derivatives in protecting X70 pipeline steel in oil well acidizing fluid: experimental and quantum chemical studies. *Journal of the Iranian Chemical Society*, 19 (6), 2331-2346.

Iroha N. B., Dueke-Eze C. U., James A. O., Fasina T. M. (2021) Newly synthesized N-(5-nitro-2-hydroxybenzylidene) pyridine-4-amine as a high-potential inhibitor for pipeline steel corrosion in hydrochloric acid medium. *Egypt J Pet* 30, 55–61. https://doi.org/10.1016/j.ejpe.2021.02.003

Iroha N. B., Madueke N. A. (2018) Effect of Triumfetta rhomboidea Leaves Extract on the Corrosion Resistance of Carbon Steel in Acidic Environment. *Chemical Science International Journal* 25 (2), 1-9

Iroha N. B., Maduelosi N. J., Nnanna L. A. (2023) The impact of tizanidine on E24 carbon steel corrosion inhibition in oilfield acidizing solution: experimental and quantum chemical studies. *Emergent Materials*, 6 (1), 137-146

Iroha N. B., Nnanna L. A. (2020) Leucas martinicensis as an inhibitor of carbon steel corrosion in acidic medium. *International Journal of Research* 7, 19-26

Iroha N.B., Nnanna L.A., (2021) Tranexamic Acid as Novel Corrosion Inhibitor for X60 Steel in Oil Well Acidizing Fluids: Surface Morphology, Gravimetric and Electrochemical Studies. *Prog Color Colorants Coat* 14, 1-11.

Iroha N.B., Nnanna L.A., Maduelosi N.J., *et al*. (2022) Evaluation of the anticorrosion performance of Tamsulosin as corrosion inhibitor for pipeline steel in acidic environment: experimental and theoretical study. *J Taibah Univ Sci* 16(1), 288–299. https://doi.org/10.1080/16583655.2022.2048512

James A. O., Iroha N. B. (2019) An Investigation on the Inhibitory Action of Modified Almond Extract on the Corrosion of Q235 Mild Steel in Acid Environment. *IOSR J. Appl. Chem*., 12, 1-10

James A.O. Iroha N. B. (2022). New green inhibitor of Olax subscorpioidea root for J55 carbon steel corrosion in 15% HCl: theoretical, electrochemical, and surface morphological investigation. *Emergent Materials*. 5 (4), 1119-1131. https://doi.org/10.1007/s42247-021-00161-1

Ji G., Anjum S., Sundaram S., Prakash R. (2015) Musa paradisica peel extract as green corrosion inhibitor for mild steel in HCl solution. *Corros. Sci*., 90, 107–117.

Kassem M.E., Ibrahim L.F., Hussein S.R., El-Sharawy R., El-Ansari M.A., Hassanane M.M., Booles H.F. (2016) Myricitrin and bioactive extract of Albizia amara leaves: DNA protection and modulation of fertility and antioxidant-related genes expression. *Pharm Biol.,* 11, 2404-2409.

Keramatinia M., Ramezanzadeh B., Mahdavian M. (2019) Green production of bioactive components from herbal origins through one-pot oxidation/polymerization reactions and application as a corrosion inhibitor for mild steel in HCl solution. *J. Taiwan Inst. Chem. Eng*. 105, 134–149.

Li T.M., Li W.K., Yu J.G. (1997) Flavonoids from Artabotrys hexapetalus. *Phytochemistry.* 45, 831-833

Lin L.Z., Lu S., Harnly J.M. (2007) Detection and quantification of glycosylated flavonoid malonates in celery, Chinese celery, and celery seed by LC-DAD-ESI/MS. *J. Agric. Food Chem.* 55, 1321-1326

Lrhoul H., Sekkal H., Hammouti B. (2023) Natural Plants as Corrosion Inhibitors: Thermodynamic's restrictions, *Mor. J. Chem.*, 11(3), 689-698, https://doi.org/10.48317/IMIST.PRSM/morjchem-v11i3.40144

Marzouk, M.M., Hussein, S.R., Kassem, M.E.S., *et al*. (2016) Phytochemical constituents and chemosystematic significance of Chrozophora tinctoria (L.) Raf. *Nat Prod Res.* 30(13), 1537-41.

Merimi I., Aslam R., Hammouti B., *et al*. (2021),Adsorption and inhibition mechanism of (Z)-4-((4-methoxybenzylidene)amino)-5-methyl-2,4-dihydro-3H-1,2,4-triazole-3-thione on carbon steel corrosion in HCl: Experimental and theoretical insights, *Journal of Molecular Structure*, 1231, 129901 https://doi.org/10.1016/j.molstruc.2021.129901

Merimi C., Hmada A., Hejjaj C., Almutairi S.M., Lgaz H., *et al*. (2024) Investigating the potency of new imidazolium ionic liquids in preventing carbon steel corrosion in acidic conditions: An integrated experimental and DFTB semi-empirical approach. *Inorganic Chemistry Communications*. 167, 112802.

Mohamme K.Z., Hamdy A., Abdel-Wahab A., Farid N.A. (2012) Temperature effect on corrosion inhibition of carbon steel in formation water by non-ionic inhibitor and synergistic influence of halide ions. *Life* Sci. J., 9, 424–434.

Myung N.V., Park D.Y., Yoo B.Y., Sumodjo P.T.A. (2003) Development of electroplated magnetic materials for MEMS. *J Magn Magn Mater* 265, 189–198. https://doi.org/10.1016/S0304-8853(03)00264-6

Nadi I., Belattmania Z., Sabour B., Reani A., Sahibed-dine A., Jama C., Bentiss F. (2019) Sargassum muticum extract based on alginate biopolymer as a new efficient biological corrosion inhibitor for carbon steel in hydrochloric acid pickling environment: Gravimetric, electrochemical and surface studies. *Int. J. Biol. Macromol.*, 141, 137-149, https://doi.org/10.1016/j.ijbiomac.2019.08.253.

Nahle A., Salim´R., El Hajjaji F., Aouad M. R., *et al*. (2021), Novel triazole derivatives as ecological corrosion inhibitors for mild steel in 1.0 M HCl: experimental & theoretical approach, *RSC Adv.*, 11, 4147–4162, https://doi.org/10.1039/d0ra09679b

Nwosu F. O. and Muzakir M. M. (2016). Thermodynamic and adsorption studies of corrosion inhibition of mild steel using lignin from siam weed (Whromolaena odorata) in acid medium. *J. Mater. Envir. Sci.* 7, 1663–1673.

Obruche E. K., Ogwuche C.E, Erhabor O.D. & Mkurzurum.C. (2019). Investigating the corrosion inhibition effects of tagetes erecta leaf extract on aluminium in acidic medium. *Global Scientific Journal*, 7(1), 1-17.

Raghavendra N. (2020) Green Compounds to Attenuate Aluminum Corrosion in HCl Activation: A Necessity Review. *Chem. Afr*., 3, 21–34.

Rani P. D. and Selvaraj S. (2010) Inhibitive and adsorption properties of Punica granatum extract on brass in acid media, *Journal of Phytology*, 2, 58-64, 2010.

Sanbongi C., Osakabe N., Natsume M., Takizawa T., Gomi S., Osawa T. (1998) Antioxidative polyphenols isolated from Theobroma cacao. *J. Agric. Food Chem.* 46, 454-457

Salmasifar A., Edraki M., Alibakhshi E., *et al*. (2021) Combined electrochemical/surface investigations and computer modeling of the aquatic Artichoke extract molecules corrosion inhibition properties on the mild steel surface immersed in the acidic medium. *J. Mol. Liq*. 327, 114856.

Shandukani P. D, Tshidino S.C, Masoko P. and Moganedi K.M. (2018) Antibacterial activity and in situ efficacy of Bidens pilosa Linn and Dichrostachys cinerea Wight et Arn extracts against common diarrhoea-causing waterborne bacteria. *BMC Complementary and Alternative Medicine*, 18:171. https://doi.org/10.1186/s12906-018-2230-9

Singh A., Ahamad I., Quraishi M.A. (2013) Piper longum extract as green corrosion inhibitor for aluminium in NaOH solution. Arabian Journal of Chemistry, http://dx.doi.org/10.1016/j.arabjc.2012.04.029

Udensi S. C., Ekpe, O. E., Nnanna, L. A. (2021) Corrosion inhibition performance of low cost and eco-friendly Treculia africana leaves extract on aluminium alloy AA7075-T7351 in 2.86% NaCl solutions. *Sci. Afr*., 12, e00791.

Umoren S.A., Eduok U. (2016) Application of carbohydrate polymers as corrosion inhibitors for metal substrates in different media: A review. *Carbohydr. Polym*.,140, 314–341.

Zeid A.H., Hifnawy M.S., Mohammed R.S. (2009) Phenolic Compounds and Biological Activities of Dichrostachys cinerea L., *Med Aromat Plant Sci Biotechnol.* 3, 42-49

Zhang W., Nie B., Li H. J., Li Q., Li C., Wu Y. C. (2021) Inhibition of mild steel corrosion in 1 M HCl by chondroitin sulfate and its synergistic effect with sodium alginate. Carbohydr. Polym., 260, 117842, https://doi.org/10.1016/j.carbpol.2021.117842